J Fluoresc
DOI 10.1007/s10895-015-1697-8

SHORT COMMUNICATION

SYBR Gold Fluorescence Quenching is a Sensitive Probe of Chitosan-microRNA Interactions

Beatriz Santos-Carballal[1] · **Musti J. Swamy**[2] · **Bruno M. Moerschbacher**[1] · **Francisco M. Goycoolea**[1]

Received: 5 August 2015 / Accepted: 14 October 2015

Abstract Competitive dye displacement titration has previously been used to characterize chitosan–DNA interactions using ethidium bromide. In this work, we aim to develop a fast and reliable method using SYBR Gold as a fluorescent probe to evaluate the binding affinity between ssRNA and chitosan. The interaction of chitosan with ssRNA was investigated as a function of temperature, molecular weight and degree of acetylation of chitosan, using competitive dye displacement titrations with fluorescence quenching. Affinity constants are reported, showing the high sensitivity of the interaction to the degree of acetylation of chitosan and barely dependent on the molecular weight. We propose that the mechanism of SYBR Gold fluorescence quenching is governed by both static and dynamic quenching.

Keywords Chitosan · Single-stranded RNA · Dye displacement titration · Fluorescence quenching

Introduction

Chitosans are a biodegradable and biocompatible family of cationic polysaccharides obtained by N-deacetylation of chitin and composed by D-glucosamine and N-acetyl-D-glucosamine units. The N-acetyl-D-glucosamine content in the polymer is defined by the degree of acetylation (DA) [1, 2]. Chitosan can form self-assembled electrostatic complexes through the interaction between the positively charged D-glucosamine units and the negatively charged phosphate units from nucleotides. Therefore, several reports on the use of chitosan as a gene delivery vector have arisen in the last decades [3–6]. More recently, the use of chitosan for the delivery of microRNAs has been reported [7, 8].

MicroRNAs (miRNA) are short non-coding RNAs of approximately 22 nucleotides. They are involved in many biological pathways in animals, playing a critical role in the control of cell proliferation and differentiation [9, 10]. The biogenesis of miRNAs is tightly controlled, and their dysregulation is associated with many human diseases, particularly cancer. The development of an efficient non-viral gene delivery vector is key for further studies and clinical applications. Therefore, evaluation of the binding affinity towards different vectors must be taken into account.

The DA and molecular weight of chitosan determine its binding affinity to polynucleotides [11, 12]. The strength of this interaction will influence the complex stability, physicochemical properties and biological relevance for a defined application. In general, it is desired that chitosan binds strongly enough and condenses the polynucleotides. In so doing, it protects them from degradation and transports them to the targeted cells; but at the same time, the system must be able to deliver the cargo intracellularly. Studies addressing quantitative information about the strength of the interaction between chitosans and polynucleotides have already been conducted using isothermal titration calorimetry (ITC) [12, 13] and surface plasmon resonance (SPR) [8]. As a general trend, it has been found that the DA plays a determinant role in the interaction with nucleotides, and the molecular weight has no major effect

Electronic supplementary material The online version of this article (doi:10.1007/s10895-015-1697-8) contains supplementary material, which is available to authorized users.

✉ Francisco M. Goycoolea
goycoole@uni-muenster.de

[1] Institute of Plant Biology and Biotechnology (IBBP), University of Münster, Schlossgarten 3, D-48149 Münster, Germany

[2] School of Chemistry, University of Hyderabad, Hyderabad 500046, India

Published online: 28 October 2015

[8, 12]. Up to now, only few reports account for dye displacement titrations using fluorescence spectroscopy and ethidium bromide to evaluate binding affinity of a specific cationic molecule with nucleotides [11, 14]. The interaction between the fluorescent dye (ethidium bromide) and double-helical DNA has already been studied by fluorescent correlation spectroscopy [15, 16]. However, there is a lack of standard high throughput methods to characterize the interaction between different chitosans and nucleotides. To the best of our knowledge, the influence of the DA and molecular weight of chitosan on the binding affinity to nucleotides has never been reported using dye displacement fluorescence titrations. This study would allow standardizing a robust method based on the use of readily accessible technique like fluorescence spectroscopy. Such methods are important to define the right conditions for proper gene transfection efficiency [7, 8]. Fluorescence quenching phenomena have also been used to study silver nanoparticles by fluorescent laser dyes for advancement in biomolecular labeling, fluorescence patterning, and chemotherapy in cancer treatment [17, 18].

SYBR Gold is an ultrasensitive fluorescent stain (e.g., 25–100 fold more sensitive than ethidium bromide) for the detection of nucleic acids (λ_{ex} = 495 nm, λ_{em} = 550 nm). It is a cyanine dye that exhibits >1000-fold fluorescence enhancement upon binding to nucleic acids (e.g., dsDNA, ssDNA and RNA) due to the high fluorescence quantum yield of the SYBR Gold–nucleic acid complexes [19]. To the best of our knowledge, there are no previous reports describing the displacement of SYBR Gold from its complex with nucleic acid due to the formation of new complexes with polysaccharides. Therefore, here we aim to analyze in depth the interaction between SYBR Gold-microRNA-chitosan to determine binding affinities of different chitosans towards microRNAs. To this end, we used a series of fully characterized high-purity chitosans from which the dissociation constants with ssRNA have already been reported using SPR (HDP-1.9: DA = 1.9 %, M_w = 26,100 Da; HDP-12: DA = 12 %, M_w = 25,500 Da; HDP-29: DA = 29 %, M_w = 20,200 Da; HDP-49: DA = 49 %, M_w = 18,000 Da; LDP-1.6: DA = 1.6 %, M_w = 1300 Da; LDP-11: DA = 11 %, M_w = 1200 Da; LDP-25: DA = 25 %, M_w = 1140 Da; LDP-67: DA = 67 %, M_w = 1950 Da) [8].

Experimental Section

Single-stranded microRNA hsa-miR-145-5p (5′-GUC CAG UUU UCC CAG GAA UCC CU-3′) and SYBR Gold were purchased from Biomers (Ulm, Germany) and Life Technologies (Carlsbad, CA, USA), respectively. Acetic acid, sodium acetate and sodium chloride were purchased from Sigma Aldrich (Munich, Germany).

Interactions between different chitosan and ssRNA were evaluated by fluorescence titration (competitive dye displacement). SYBR Gold was dissolved in acetate buffer (35 mM sodium acetate, pH 5.1, containing 10 mM NaCl) to reach 10× concentrated. A 10-μL aliquot of ssRNA stock solution (50 μM) was diluted in a 1-mL cuvette with 100 μL SYBR Gold. The miRNA was titrated manually with all the chitosans (0.15 g/L in acetate buffer). Fluorescence spectra were measured in the range of 500–750 nm at the excitation wavelength of 495 nm. Simultaneously, the absorbance spectrum of each solution was registered in the range of 400–600 nm at the studied temperature. The fluorescence and absorbance spectra were measured for all the chitosans at 303 K. Additionally, for CS HDP-1.9 and LDP-1.6 the spectra were also measured at 313 and 323 K.

Fluorescence spectra were recorded on a JASCO FP-6500 spectrofluorometer (Groß-Umstadt, Germany) connected to a ThermoHaake D8 thermoregulator (Karlsruhe, Germany). A single beam with a resolution of 1 nm, bandwidth 1 nm, and voltage of 450 V were used.

Absorbance spectra were recorded using a JASCO V-550 spectrophotometer (Groß-Umstadt, Germany) connected to a ThermoHaake D8 thermoregulator (Karlsruhe, Germany). A single beam with a resolution of 1 nm, and a bandwidth of 1 nm were used.

Results and Discussion

The effect of adding incremental amounts of chitosan to complexes of SYBR Gold and single-stranded microRNA hsa-miR-145-5p (5′-GUC CAG UUU UCC CAG GAA UCC CU-3′) is illustrated in Fig. 1 for representative fluorescence and absorption spectra at two different temperatures (303 and 313 K). Notice that, the addition of chitosan (HDP-1.9) to SYBR Gold-ssRNA quenches the fluorescence at 550 nm, hence reflecting the displacement of the dye from the ssRNA chain. Additional spectra are reported as supporting information (Fig. S1).

In an attempt to elucidate the mechanism governing the fluorescence quenching process, the fluorescence intensity data were firstly corrected considering the inner filter effect, according to the following relationship (Eq. 1) [20]:

$$F_{corr} = F_{obs} \cdot \text{antilog}\left(\frac{OD_{ex} + OD_{em}}{2}\right) \quad (1)$$

where, F_{obs} is the measured fluorescence and OD_{ex} and OD_{em} are the optical density at the excitation and emission wavelengths, respectively.

Fluorescence data was fitted following the Stern-Volmer equation (Eq. 2) [20]:

$$\frac{F_0}{F} = 1 + K_D[CS] = 1 + k_q\tau_0[CS] \quad (2)$$

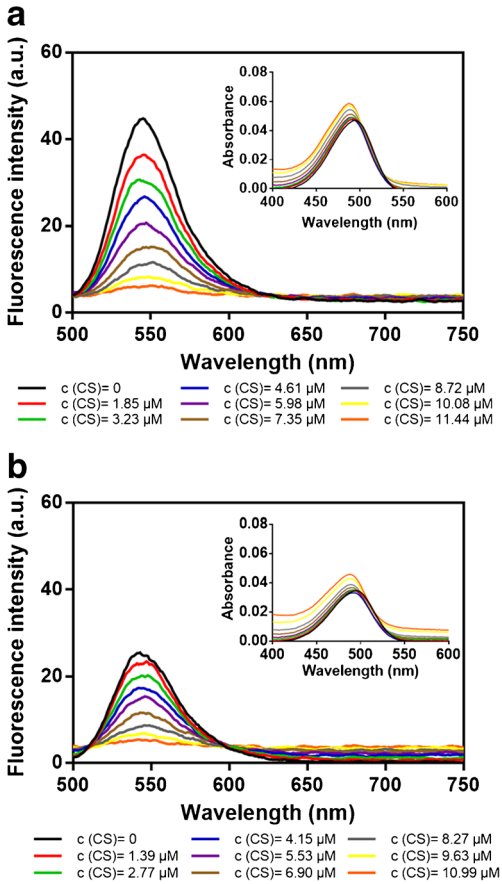

Fig. 1 Fluorescence spectra (λ_{ex} = 495 nm) of SYBR Gold-ssRNA (C_0 = 50 μM) upon titration with CS HDP-1.9 (as shown in legends) at 303 K (**a**) and 313 K (**b**) in acetate buffer (35 mM sodium acetate, pH 5.1, containing 10 mM NaCl). Insets show the corresponding absorbance spectra

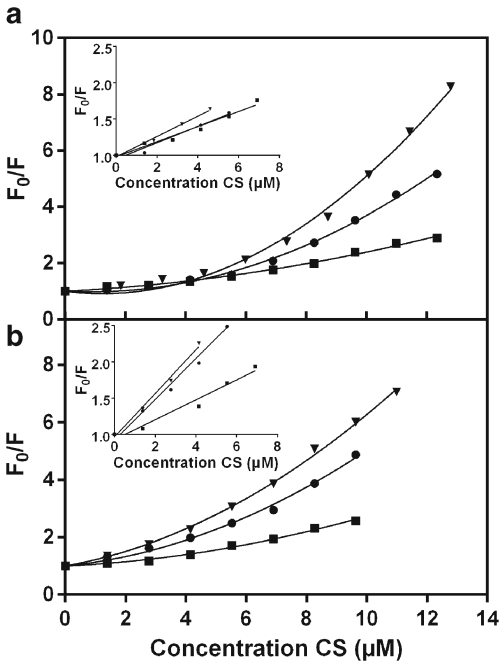

Fig. 2 Variation of the fluorescence of ssRNA-SYBR Gold complexes with concentration of added high molecular weight chitosan HDP-1.9 (**a**) and low molecular weight chitosan LDP-1.6 (**b**), at 303 K (—▼—), 313 K (—●—) and 323 K (—■—) in acetate buffer (35 mM sodium acetate, pH 5.1, containing 10 mM NaCl). Insets show the corresponding linear fit of experimental data points (Eq. 2) at low chitosan concentrations

where, F_0 and F are the fluorescence intensities after the inner filter effect correction, at initial time and at the corresponding CS concentration [CS], respectively; K_D is the dynamic quenching constant; k_q is the bimolecular quenching constant; and τ_0 is the lifetime of the fluorophore in the absence of quencher and is generally taken as 10^{-8} s [20].

Figure 2 describes the variation of the fluorescence (F_0/F) with the concentration of two types of chitosan -HDP-1.9 and LDP-1.6- at different temperatures. The linear fits from Eq. 2 are represented as inset in Fig. 2 and the values of the constants are reported in Table 1. The results showed values of the bimolecular quenching constant larger than 2×10^{10} L/mol·s, which is the maximum value permitted for collisional quenching process. In addition, it is reported that titration studies at different temperatures could be used to distinguish the mechanism of quenching at play, even though lifetime experiments are more robust [20]. Notice that in both cases the increase in the temperature decreases the fluorescence quenching. This phenomenon is characteristic of static quenching, where at higher temperatures the dissociation of complexes with lower affinity is more likely to occur, resulting in a reduction of the static quenching. This effect could be the expected consequence of the formation of a non-fluorescent ground state complex between ssRNA and chitosan. During the addition of chitosan and the displacement of SYBR Gold, the formed complex absorbs light, but it returns to the ground state without the emission of a photon. However, the mechanism cannot exclusively be attributed to static quenching. Indeed, the shape of the curves describes an upward curvature towards the *y*-axis at increasing concentrations of chitosan. This non-linear dependence could be diagnostic of combined dynamic and static quenching. In this case, the remaining fluorescence upon addition of chitosan is affected by the complexes formed and the collisional encounters.

One additional method that has been used to distinguish static and dynamic quenching is by careful examination of the absorption spectra of the fluorophore (insets Fig. 1). Collisional quenching only affects the excited states of the fluorophores, and thus, no changes in the absorption spectra are expected. In contrast, the ground-state complex formation will frequently result in perturbation of the absorption spectrum of the fluorophore, as it is observed in Fig. 1. Therefore, it is required to combine both, static and dynamic fluorescence quenching, to fully describe the behavior. To this end, we used a second order equation in chitosan concentration [CS] using

Table 1 Quenching constants from Stern-Volmer equation (Eq. 2) for CS HDP-1.9 and LDP-1.6 at different temperatures

System	T (K)	K_D (× 10^5 L/mol)	k_q (× 10^{13} L/mol·s)	R^2
ssRNA-HDP-1.9	303	1.40	1.40	0.992
	313	1.13	1.13	0.968
	323	1.04	1.04	0.966
ssRNA-LDP-1.6	303	3.00	3.00	0.992
	313	2.81	2.81	0.988
	323	1.37	1.37	0.965

the modified form of the Stern-Volmer equation (Eq. 3) [20]:

$$\frac{F_0}{F} = 1 + (K_D + K_S)[CS] + K_D K_S [CS]^2 \quad (3)$$

where, K_D and K_S are the dynamic and static quenching constants, respectively.

Altogether, the above observations suggest that the fluorescence quenching of SYBR Gold-ssRNA by chitosan is due to static quenching at low concentrations of chitosan, whereas at higher concentrations quenching mechanism involves both static and collisional components.

Although the mechanism is not completely elucidated, as long as the fluorescence signal changes, the SYBR Gold displacement titrations can be used to characterize the binding affinity. To this end, we conducted fluorescence titrations using a series of chitosans previously prepared in our laboratory. These studies have helped us to glean further understanding of the effect of the DA and Mw of chitosan on the chitosan-miRNA interaction and transfection efficiency [8].

The evaluation of the binding constants was determined using the double logarithmic plot of the Stern-Volmer equation (Eq. 4) [21]:

$$\log \frac{F_0 - F}{F} = \log K_a + n \log[CS] \quad (4)$$

where, K_a is the binding affinity constant and n is the number of binding sites assuming "infinite" cooperativity (Table 2).

Table 2 Binding parameters of different chitosans in complexes with hsa-miR-145-5p: Affinity constant ($\mathbf{K_a}$) and number of binding sites of the reaction (**n**)

Sample	$\log K_a \pm SD$	n±SD	R^2
HDP-1.9	14 ± 1	2.7 ± 0.2	0.979
HDP-12	10.5 ± 0.6	1.9 ± 0.1	0.987
HDP-29	7.3 ± 0.4	1.38 ± 0.08	0.987
HDP-49	6.7 ± 0.3	1.35 ± 0.05	0.995
LDP-1.6	9.7 ± 0.3	1.80 ± 0.05	0.996
LDP-11	8.2 ± 0.4	1.57 ± 0.07	0.990
LDP-25	6.5 ± 10.4	1.20 ± 0.08	0.984
LDP-67	7.6 ± 0.2	1.60 ± 0.04	0.996

The affinity of CS-HDP for ssRNA declines with increasing DA. CS-LDP-ssRNA systems followed the same trend except LDP-67. HDP chitosans show a higher affinity for ssRNA than do LDP chitosans and a greater dependence on the DA. The values of the number of binding sites (n) were invariably greater than 1.0 for all the chitosans, diagnostic of positive cooperative binding. These results could indicate that ssRNA binding is dependent on the DA of chitosan, although more so, in the case of high-molecular-weight chitosan molecules. This dependence possibly reflects the positive cooperative binding of high-molecular-weight chitosans as suggested previously by the SPR spectroscopy data of the same systems [8]. In turn, low-molecular weight chains exhibit overall lower cooperativity, presumably due to the far shorter chain length and hence, fewer stretches with the required cooperative length.

Figure 3 shows the affinity constants, determined by fluorescence spectroscopy, compared to the dissociations constants (K_D), determined by SPR, for the same systems in our accompanying study [8]. The results of both techniques are diagnostic that HDP chitosans show a higher affinity for ssRNA than do LDP chitosans and the DA exhibits a greater effect on binding to ssRNA.

To the best of our knowledge, this is the first account of the interaction between miRNA and chitosans as quantified by fluorescence displacement titrations using SYBR Gold. The complexes with higher content of acetylated units present a decrease in the binding constant upon interaction with ssRNA.

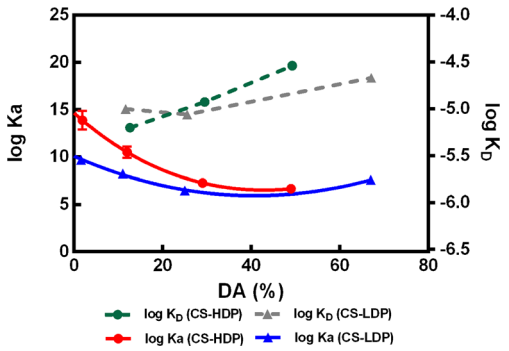

Fig. 3 Dependence of the affinity constants (Ka) calculated from Stern-Volmer equation (Eq. 4), and dissociation constants (K_D) determined by SPR [8], with degree of acetylation and degree of polymerization of chitosans upon interaction with ssRNA

This result could be explained by the differences in the charge density of chitosan polyelectrolytes, in which higher amount of polymer is required to reach the same number of protonated D-glucosamine units. Similar systems have already been studied using ITC for evaluating the binding parameters of chitosan during its interaction with pDNA and siRNA [12, 13]. It was shown for chitosan–pDNA interactions that the DA has an influence on the structure and stability of the complexes formed. Chitosans with lower DA involve less number of chains to saturate the binding sites of pDNA [12]. For complexes formed between chitosan and siRNA no significant increase in binding affinity for higher molecular weight chitosans was reported by ITC [13].

Conclusions

Fluorescence spectroscopy is a technique frequently used to study dye displacement titrations. Changes in the fluorescence intensity of a dye-ssRNA complex upon addition of chitosan can be exploited to derive values of affinity constants along with information about the number of binding sites available for the interaction. Here, we used SYBR Gold as an external displacement dye in fluorescent titrations. The high sensitivity of the SYBR Gold probe allowed us to implement an analytical method to evaluate the strength of the interaction between different chitosans and microRNA (ssRNA). The fluorescence quenching mechanism is governed by both dynamic and static quenching. The degree of acetylation of chitosan plays a major role in the interaction with microRNA, and this effect is more remarkable for high molecular weight chitosan, confirming the results previously found by SPR [8].

Acknowledgments We acknowledge financial support and a PhD fellowship to BSC from German Research Council DFG (Project GRK 1549 International Research Training Group 'Molecular and Cellular Glyco-Sciences'); from The Danish Agency for Science, Technology and Innovation, Denmark (FENAMI project 10-093456); the research leading to these results has also received funding from the European Union's Seventh Framework Program for research, technological development and demonstration under grant agreement n° 613931. We are indebted to Prof. Susanne Fetzner (University of Münster), for her generous access to spectrophotometer and spectrofluorometer instruments. We thank Dr. Juan Pablo Fuenzalida and Dr. Kishore Babu Bobbili for their support during the experiments.

References

1. Rinaudo M (2006) Chitin and chitosan: properties and applications. Prog Polym Sci 31:603–632. doi:10.1016/j.progpolymsci.2006.06.001
2. Harish Prashanth KV, Tharanathan RN (2007) Chitin/chitosan: modifications and their unlimited application potential—an overview. Trends Food Sci Technol 18:117–131. doi:10.1016/j.tifs.2006.10.022
3. Liu X, Howard KA, Dong M, et al. (2007) The influence of polymeric properties on chitosan/siRNA nanoparticle formulation and gene silencing. Biomaterials 28:1280–1288. doi:10.1016/j.biomaterials.2006.11.004
4. Lavertu M, Méthot S, Tran-Khanh N, Buschmann MD (2006) High efficiency gene transfer using chitosan/DNA nanoparticles with specific combinations of molecular weight and degree of deacetylation. Biomaterials 27:4815–4824. doi:10.1016/j.biomaterials.2006.04.029
5. Ragelle H, Vandermeulen G, Préat V (2013) Chitosan-based siRNA delivery systems. J Control Release 172:207–218. doi:10.1016/j.jconrel.2013.08.005
6. Koping-Hoggard M, Tubulekas I, Guan H, et al. (2001) Chitosan as a nonviral gene delivery system. Structure-property relationships and characteristics compared with polyethylenimine in vitro and after lung administration in vivo. Gene Ther 8:1108–1121. doi:10.1038/sj.gt.3301492
7. McKiernan PJ, Cunningham O, Greene CM, Cryan S-A (2013) Targeting miRNA-based medicines to cystic fibrosis airway epithelial cells using nanotechnology. Int J Nanomedicine 8:3907–3915. doi:10.2147/IJN.S47551
8. Santos-Carballal B, Aaldering LJ, Ritzefeld M, et al. (2015) Physicochemical and biological characterization of chitosan-microRNA nanocomplexes for gene delivery to MCF-7 breast cancer cells. Sci Rep 5:13567. doi:10.1038/srep13567
9. Adammek M, Greve B, Kässens N, et al. (2013) MicroRNA miR-145 inhibits proliferation, invasiveness, and stem cell phenotype of an in vitro endometriosis model by targeting multiple cytoskeletal elements and pluripotency factors. Fertil Steril 99:1346–1355e5. doi:10.1016/j.fertnstert.2012.11.055
10. Götte M, Mohr C, Koo C-Y, et al. (2010) MiR-145-dependent targeting of Junctional Adhesion Molecule A and modulation of fascin expression are associated with reduced breast cancer cell motility and invasiveness. Oncogene 29:6569–6580. doi:10.1038/onc.2010.386
11. Liu W, Sun S, Cao Z, et al. (2005) An investigation on the physicochemical properties of chitosan/DNA polyelectrolyte complexes. Biomaterials 26:2705–2711. doi:10.1016/j.biomaterials.2004.07.038
12. Ma PL, Lavertu M, Winnik FM, Buschmann MD (2009) New insights into chitosan-DNA interactions using isothermal titration microcalorimetry. Biomacromolecules 10:1490–1499. doi:10.1021/bm900097s
13. Holzerny P, Ajdini B, Heusermann W, et al. (2012) Biophysical properties of chitosan/siRNA polyplexes: profiling the polymer/siRNA interactions and bioactivity. J Control Release 157:297–304. doi:10.1016/j.jconrel.2011.08.023
14. Wiethoff CM, Gill ML, Koe GS, et al. (2003) A fluorescence study of the structure and accessibility of plasmid DNA condensed with cationic gene delivery vehicles. J Pharm Sci 92:1272–1285. doi:10.1002/jps.10391
15. Magde D, Elson E, Webb WW (1972) Thermodynamic fluctuations in a reacting system—measurement by fluorescence correlation spectroscopy. Phys Rev Lett 29:705–708. doi:10.1103/PhysRevLett.29.705
16. Magde D, Elson EL, Webb WW (1974) Fluorescence correlation spectroscopy. II. An experimental realization. Biopolymers 13:29–61. doi:10.1002/bip.1974.360130103
17. Mastiholi BM, Tangod VB, Raikar US (2013) Influence of metal nanoparticles on ADS560EI fluorescent laser dye. Opt Int J Light Electron Opt 124:261–264. doi:10.1016/j.ijleo.2011.11.054
18. Tangod VB, Raikar P, Mastiholi BM, Raikar US (2014) Solvent polarity studies of highly fluorescent laser dye ADS740WS and its fluorescence quenching with silver nanoparticles. Can J Phys 92:116–123. doi:10.1139/cjp-2013-0250

19. Tuma RS, Beaudet MP, Jin X, et al. (1999) Characterization of SYBR gold nucleic acid gel stain: a dye optimized for use with 300-nm ultraviolet transilluminators. Anal Biochem 268:278–288. doi:10.1006/abio.1998.3067
20. Lakowicz JR (2006) Principles of fluorescence spectroscopy. Springer US, United States
21. Yu X, Liu R, Yi R, et al. (2011) Study of the interaction between N-confused porphyrin and bovine serum albumin by fluorescence spectroscopy. Spectrochim Acta A Mol Biomol Spectrosc 78: 1329–1335. doi:10.1016/j.saa.2011.01.024